

# Thermodynamics of quantum oscillators

Michel Caffarel<sup>1,\*</sup>

<sup>1</sup>*Laboratoire de Chimie et Physique Quantiques (UMR 5626), CNRS and Université de Toulouse, France*

In this work, we present a compact analytical approximation for the quantum partition function of systems composed of quantum oscillators. The proposed formula is general and applicable to an arbitrary number of oscillators described by a rather general class of potential energy functions (not necessarily polynomials). Starting from the exact path integral expression of the partition function, we introduce a time-dependent Gaussian approximation for the potential contribution and, then, invoke a principle of minimal sensitivity to minimize the error. This leads to a system of coupled nonlinear equations whose solution yields the optimal parameters of the gaussian approximation. The resulting approximate partition function accurately reproduces thermodynamic quantities such as the free energy, average energy, and specific heat -even at zero temperature- with typical errors of only a few percent. We illustrate the performance of our approximate formula with numerical results for systems of up to ten coupled anharmonic oscillators. These results are compared to "exact" numerical results obtained via Hamiltonian diagonalization for small systems and Path Integral Monte Carlo simulations for larger ones.

## I. INTRODUCTION

Quantum oscillators play a central role in a variety of scientific domains. Prominent applications include molecular vibrations,[1] phonons in solids,[2] and quantum field theory (theory of light[3],  $\phi^4$ -theory,[4], etc.). However, many other fields make use of quantum oscillators such as nonlinear optical phenomena,[3], quantum decoherence, [5], qubits in superconducting circuits,[6] etc. The governing equations of these systems being nonlinear and, in general, non-integrable, quantum oscillators also provide a versatile framework for investigating fascinating phenomena such as, *e.g.*, quantum chaos[7] or mixed classical-quantum behavior.[8] Moreover, they serve as standard models for the development and validation of computational and analytical techniques in applied mathematics, such as perturbation theory, numerical diagonalization, variational methods, and semiclassical approximations. A quantitative understanding of their quantum properties is therefore important.

Here, we address the problem of evaluating the partition function (PF) for a general system of  $N$  quantum oscillators. No specific restrictions on the form of the potential energy function are introduced and, in principle, arbitrary anharmonicities and couplings between oscillators can be considered. As is well known, the partition function is the fundamental quantity of equilibrium thermodynamics, from which key properties such as internal energy, entropy, and specific heat can be derived. The quantum partition function is defined as

$$Z(\beta) = \text{Tr} e^{-\beta H} \quad (1)$$

where  $\beta$  denotes the inverse temperature ( $\beta = \frac{1}{k_B T}$ ),  $H$  is the Hamiltonian operator, and  $\text{Tr}$  indicates the trace over the Hilbert space.

Evaluating the partition function in the general case is a formidable challenge. For small systems, accurate numerical values of the PF (at least, for not too high values of the temperature) can be obtained by explicitly summing over the contributions of individual energy levels, using  $Z = \sum_i e^{-\beta E_i}$ . This approach requires numerical determination of the energy spectrum -a task which is feasible only for systems with a limited number of oscillators because of the exponential growth of the Hilbert space with system dimensionality. Among the various strategies developed to compute accurate energy levels for larger systems, the Discrete Variable Representation (DVR) method[9, 10] has proven particularly effective. Nevertheless, extending DVR to systems with more than a dozen of oscillators remains challenging. In recent years, Density Matrix Renormalization Group (DMRG) techniques[11] have gained considerable attention, achieving remarkable success in high-dimensional systems; notably, applications involving up to 24 coupled vibrational modes have been reported.[12] Despite these advances, both DVR and DMRG require the calculation of a potentially large number of energy levels with high precision, particularly at high temperature, thus limiting their applicability to large-scale problems.

For systems composed of a large number of oscillators, a powerful alternative is to evaluate the partition function by using its path integral representation, as introduced by Feynman.[13] In this formalism, the PF is expressed as a sum over an infinite set of paths

$$Z(\beta) = \int \mathcal{D}[\mathbf{x}(t)] e^{-S[\mathbf{x}(t)]}, \quad (2)$$

where  $S$  denotes the Euclidean (imaginary-time) action corresponding to the Hamiltonian and the notation  $\int \mathcal{D}[\mathbf{x}(t)] \dots$  indicates the functional integration, that is, a summation over all possible paths  $\mathbf{x}(t)$  evolving from  $t = 0$  to  $t = \beta$ . Here,  $\mathbf{x}(t)$  denotes the  $N$ -dimensional vector of displacements of each of the  $N$  oscillators at time  $t$ .

\* caffarel@irsamc.ups-tlse.fr

In practice, this path integral cannot be evaluated analytically, except for simple cases such as the free particle, the harmonic oscillator, and the hydrogen atom (see, [14]). A standard route is thus to resort to numerical approaches. To that end, the continuous paths are discretized into  $n$  time slices, with  $\beta = n\tau$ ,  $\tau$  being the discretized imaginary time step. A path is thus represented by the discretized sequence  $\mathbf{x}(t) = [\mathbf{x}(0), \dots, \mathbf{x}(i\tau), \dots, \mathbf{x}(\beta = n\tau)]$ . In the literature, the integer  $n$  is commonly referred to as the number of beads or Trotter number. After discretization, the PF is rewritten as an ordinary  $nN$ -dimensional integral

$$Z_n(\beta) = \int \prod_{i=1}^n \prod_{k=1}^N dx_k^i e^{-S_n(\mathbf{x}, \tau)} \quad (3)$$

where  $x_k^i$  is the displacement of the  $k$ -th oscillator at the  $i$ -th time slice and  $S_n$  the discretized version of  $S$ . The exact value of the partition function is recovered in the limit  $n \rightarrow \infty$ , corresponding to an infinite-dimensional integral. Evaluating such high-dimensional integrals is feasible in practice only through stochastic sampling techniques or molecular dynamics simulations, leading to the two most widely used numerical approaches: Path Integral Monte Carlo (PIMC) [15] and Path Integral Molecular Dynamics (PIMD) [16, 17], respectively. Both methods are numerically "exact", meaning they systematically converge to the correct result as the number of beads  $n$  increases and statistical or sampling errors vanish. However, for large systems, their practical implementation can be computationally very demanding, due to the need to reduce statistical or sampling errors to acceptable levels and, also, to use a sufficiently large number of beads, particularly at low temperatures.

In this work, we start from the path integral representation of the partition function, Eq. (3). Rather than performing a direct numerical evaluation of the resulting high-dimensional integral, we propose an analytical approximation scheme that yields an explicit, closed-form expression for the partition function. Remarkably, as demonstrated in the applications presented below, the error in both the partition function and the derived thermodynamic quantities appears to be small (what we mean here by small will be precised below) when compared to reference results obtained via "exact" numerical calculations for small systems or Path Integral Monte Carlo (PIMC) simulations for larger ones.

The present work extends earlier studies for the single anharmonic quartic oscillator with potential  $V(x) = \frac{1}{2}\omega^2 x^2 + gx^4$  [18, 19] to the general case of arbitrarily many oscillators with general coupling and anharmonicity. In the one-dimensional case, our approximate partition function was found to be both qualitatively and quantitatively faithful to the exact result. Notably, it correctly reproduces the exact high-temperature (classical) limit  $\beta \rightarrow 0$ , the harmonic limit  $g \rightarrow 0$ , and yields accurate functional forms with precise coefficients in both the weak-coupling ( $g$  small) and strong-coupling

( $g$  large) regimes. In particular, the approach captures the factorial-like divergence characteristic of the weak-coupling expansion, [20, 21] as well as the behavior of the low-lying energy levels as a function of the anharmonicity parameter  $g$ . Quantitatively, the errors in the computed ground- and excited-state energies typically remain within a few percent. These promising results provided strong motivation to generalize the method to multi-dimensional systems, which is the focus of the present work.

To help clarify the approach presented in this work, it is worthwhile in this introduction to briefly summarize the key steps leading to our original formula. The full mathematical details will be provided in the next section.

Following the standard route, the partition function, Eq. (3), may be expressed as an integral over a product of short-time (high-temperature) propagators, each including a kinetic contribution and a potential term of the form  $e^{-\tau V(\mathbf{x})}$  where  $V$  denotes the total potential. Our central approximation consists in replacing, at each time slice of the path integral, the exact potential by a quadratic approximation,  $V_G$ . More precisely, the replacement reads

$$\frac{e^{-\tau V(\mathbf{x})}}{\int d\mathbf{x} e^{-\tau V(\mathbf{x})}} \rightarrow \frac{e^{-\tau V_G(\mathbf{x}, \tau)}}{\int d\mathbf{x} e^{-\tau V_G(\mathbf{x}, \tau)}} \quad (4)$$

where the quadratic potential is chosen under the following general form

$$V_G(\mathbf{x}, \tau) = \frac{1}{2} \sum_{k=1}^N \omega_{gk}^2(\tau) x_k^2 + b_{gk}(\tau) x_k + \sum_{k<l} K_{gkl}(\tau) x_k x_l, \quad (5)$$

where  $K$  is a matrix chosen symmetric without loss of generality. Here, the quantities  $[\omega_{gk}(\tau), b_{gk}(\tau)]$  for  $k = 1$  to  $N$  and  $K_{gkl}(\tau)$  for  $k < l$  play the role of fitting parameters. Note that a distinct set of parameters is associated with each value of the time step. The parameters will be chosen so as to minimize the approximation error. Let us emphasize that the quadratic potential depends explicitly on the time-step  $\tau$  via the fitting parameters. This must be contrasted with what is done in more conventional approaches -such as mean-field-like methods- where the Hamiltonian and the action are made quadratic from the start, independently of  $\tau$ . A second remark is that the Gaussian approximation is applied to *normalized* distributions, see Eq. (4). As will become clear later, considering normalized quantities for  $e^{-\tau V}$  and  $e^{-\tau V_G}$  is important to get an accurate PF. To determine the optimal fitting parameters for a given  $\tau$  some freedom is available. Here, we propose to set the parameter values by imposing the equality of the first and second moments of the exact and Gaussian distributions involved in Eq. (4).

After applying the Gaussian approximation, the path integral reduces to that of a system of coupled harmonic oscillators. The PF can thus be evaluated analytically,

leading to an expression of the form

$$Z_n = \left[ \frac{I(\tau)}{I_G(\tau)} \right]^n Z_n^H[\omega_{gk}(\tau), b_{gk}(\tau), K_{gkl}(\tau)] \quad (6)$$

where  $I(\tau)$  and  $I_G(\tau)$  are the normalization of the exact and Gaussian distributions, respectively, that is

$$I(\tau) = \int d\mathbf{x} e^{-\tau V}, \quad (7)$$

$$I_G(\tau) = \int d\mathbf{x} e^{-\tau V_G}, \quad (8)$$

and  $Z_n^H$  is the analytically known partition function of the corresponding approximate *harmonic* system. At this point, the next step should consist as usual in taking the  $n \rightarrow \infty$  limit. However, it is not possible here because of the presence in Eq.(6) of the prefactor  $\left[ \frac{I(\tau)}{I_G(\tau)} \right]^n$  which either diverge or vanish in this limit. For the case of the one-dimensional quartic oscillator,[18, 19] we have proposed not to take this limit and, instead, to evaluate the partition function at some *finite* value of  $n$  or, equivalently,  $\tau$ . For each  $\beta$ , the value of  $n$  is chosen to be the value which minimizes the sensitivity of the partition function to the Gaussian approximation. In the 1d-quartic case where there is only a single fitting parameter  $\omega_g$  ( $b_g = 0$  by symmetry and  $K_{gkl} = 0$ ) this *Principle of Minimal Sensitivity* (PMS) amounts to imposing

$$\frac{\partial Z_n}{\partial \omega_g(\tau)} = 0. \quad (9)$$

As shown in [18], this equation admits a unique solution, denoted  $n_c(\beta)$  (and, equivalently, a unique time step  $\frac{\beta}{n_c(\beta)}$ ). We have then proposed the final expression of the partition function to be

$$\mathcal{Z}(\beta) = Z_{n_c(\beta)}. \quad (10)$$

It is worth noting that this principle of minimal sensitivity is not new. It has been introduced in various contexts by several authors (see, e.g., [22], [23], [24], [25]). It is both a general and natural principle: When approximating a quantity by an expression  $Q(\mathbf{p})$  that depends on some *unphysical* parameters  $\mathbf{p}$ , a reasonable criterion for selecting the "best" parameters is to minimize the sensitivity of the approximation to these parameters, that is, imposing  $\frac{\partial Q}{\partial \mathbf{p}} = 0$ .

Here, for the case of general oscillators, we extend the application of the principle of minimal sensitivity to each of the fitting parameters,  $[\omega_{gk}(\tau), b_{gk}(\tau), K_{gkl}(\tau)]$ . As we will show, the resulting so-called PMS equations, together with those obtained from the matching of the first and second moments of the exact and Gaussian normalized distributions [Eq. (4)], result in a system of coupled nonlinear equations involving multiple time steps (essentially, one time step per fitting parameter). Solving iteratively this system allows us to determine the values of the time steps and, thus, the partition function.

The organization of the paper is as follows. In Section II, we present the full derivation of our partition function in detail. Section III is devoted to some numerical applications. We begin with small systems ( $N = 1, 2$ , and 3 oscillators) for which the exact partition function can be known numerically with high accuracy. We then move on to a system of coupled quartic oscillators of increasing size, up to  $N = 10$ . The results obtained with our model partition function are compared to those from path integral Monte Carlo (PIMC) simulations. Finally, in Section IV, we present some concluding remarks and perspectives.

## II. THEORY

In this work, we consider the following Hamiltonian for a system of  $N$  quantum oscillators

$$H = -\frac{1}{2} \sum_{k=1}^N \frac{\partial^2}{\partial x_k^2} + V(\mathbf{x}), \quad (11)$$

where  $x_k$  denotes the displacement of the  $k$ -th oscillator from equilibrium,  $V(\mathbf{x})$  is the total potential energy, and  $\mathbf{x} = (x_1, \dots, x_N)$  the vector of displacements. Note that the coordinates  $x_k$  may have been previously rescaled to absorb the oscillator masses, making all masses equal to one without loss of generality. In this work, we will consider potential functions that involve only pairwise couplings between oscillators. More precisely, we consider potentials of the form

$$V(\mathbf{x}) = \sum_{k=1}^N V_k(x_k) + \sum_{1 \leq k < l \leq N} V_{kl}(x_k, x_l). \quad (12)$$

In fact, much of the theory remains valid for more general coupling schemes and can be extended without significant difficulty. However, to avoid unnecessary complications in the exposition, we postpone the presentation of such extensions to future work. No specific constraints are imposed on the analytical form of the potential energy. However, we require  $V$  to be bounded from below and  $V \rightarrow +\infty$  as  $|\mathbf{x}| \rightarrow \infty$ . These conditions are standard for generic oscillators; they lead to a discrete energy spectrum. However, they exclude cases where oscillations can be unbounded, such as for the Morse oscillator.[26, 27] In the illustrative simulations to follow, we will use a standard polynomial form of order 4 for the potential, namely  $V = \sum_{k,l} c_{kl} x_k^m x_l^n$  with  $m + n \leq 4$ , but we insist that non-polynomial forms can also be considered.

In order to derive our fundamental formula, we start from the exact path integral representation of the partition function,[13]

$$Z(\beta) = \lim_{n \rightarrow \infty} Z_n(\beta) \quad (13)$$

with

$$Z_n(\beta) = \left( \frac{1}{\sqrt{2\pi\tau}} \right)^{nN} \int \prod_{i=1}^n \prod_{k=1}^N dx_k^i$$

$$e^{-\frac{1}{\tau} \sum_{i,j} \sum_{k=1}^N x_k^i A_{ij} x_k^j - \tau \sum_{i=1}^n V(\mathbf{x}^i)} \quad (14)$$

Here,  $\beta$  is the inverse temperature,  $n$  the number of beads,  $\tau$  the time-step equal to  $\tau = \frac{\beta}{n}$ ,  $x_k^i$  the displacement of the  $k$ -th oscillator at time  $t_i = i\tau$ , and  $\mathbf{x}^i = (x_1^i, \dots, x_N^i)$ .  $A$  is the matrix associated with the kinetic part; it is given by

$$A_{ij} = \delta_{ij} - \frac{1}{2}(\delta_{i+1,j} + \delta_{i-1,j}) \quad (15)$$

with  $A_{1n} = A_{n1} = -\frac{1}{2}$  (periodic boundary conditions in time).

As mentioned in the introduction, the first key step of the approach consists in introducing a gaussian approximation for the quantity  $e^{-\tau V(\mathbf{x}^i)}$  at each time slice. Using the notations defined in the introduction the approximation writes

$$e^{-\tau V(\mathbf{x})} \simeq \frac{I(\tau)}{I_G(\tau)} e^{-\tau V_G(\mathbf{x}, \tau)} \quad (16)$$

where the quadratic potential  $V_G$  is given by Eq.(5). The total number of fitting parameters in  $V_G$  is equal to  $2N + \frac{N(N-1)}{2}$ . For a given  $\tau$ , we propose to determine the fitting parameters by imposing the equality of the first and second moments of the normalized distributions associated with the exact and quadratic potential,  $\pi \equiv e^{-\tau V} / \int d\mathbf{x} e^{-\tau V}$  and  $\pi_G \equiv e^{-\tau V_G} / \int d\mathbf{x} e^{-\tau V_G}$ , respectively

$$\langle x_k \rangle_\pi = \langle x_k \rangle_{\pi_G} \quad (17)$$

and

$$\langle x_k x_l \rangle_\pi = \langle x_k x_l \rangle_{\pi_G} \quad (18)$$

for  $k, l = 1$  to  $N$  and  $k < l$ . Here, the average over  $\pi$  of a function  $f$  is defined as usual as

$$\langle f \rangle_\pi = \int d\mathbf{x} f(\mathbf{x}) \pi(\mathbf{x}), \quad (19)$$

with a similar formula for the gaussian average,  $\langle f \rangle_{\pi_G}$ . Equations (17, 18) constitute a system of  $M$  equations with  $M$  unknowns, where  $M$  represents the number of fitting parameters to be determined. To solve this system, we begin by expressing the Gaussian distribution  $\pi_G$  in the following form:

$$\pi_G = \frac{e^{-\frac{1}{2}(\mathbf{x}, A\mathbf{x}) - B\mathbf{x}}}{\int d\mathbf{x} e^{-\frac{1}{2}(\mathbf{x}, A\mathbf{x}) - B\mathbf{x}}} \quad (20)$$

Here, the matrix and vector components are defined as  $A_{kl} = \tau(\omega_{gk}^2 \delta_{kl} + K_{gkl})$  and  $B_k = \tau b_{gk}$ , respectively. For a Gaussian distribution written in this canonical form, it is well known that the mean is given by

$$\langle x_k \rangle_{\pi_G} = -(A^{-1}B)_k \quad (21)$$

and the covariance matrix given by

$$\langle (x_k - \langle x_k \rangle_{\pi_G})(x_l - \langle x_l \rangle_{\pi_G}) \rangle_{\pi_G} = A_{kl}^{-1} \quad (22)$$

Putting together Eqs.(17,18,21,22) we get the explicit  $\tau$ -dependence of the fitting parameters as follows

$$\omega_{gk}(\tau) = \sqrt{\frac{C_{kk}^{-1}(\tau)}{\tau}} \quad (23)$$

$$K_{gkl}(\tau) = \frac{C_{kl}^{-1}(\tau)}{\tau} \quad (24)$$

and

$$b_{gk}(\tau) = -\frac{1}{\tau} \sum_{l=1}^N C_{kl}^{-1}(\tau) \mu_l(\tau) \quad (25)$$

where  $C$  and  $\mu$  are the exact covariance matrix,  $C_{kl}(\tau) = \langle (x_k - \langle x_k \rangle_\pi)(x_l - \langle x_l \rangle_\pi) \rangle_\pi$ , and exact mean,  $\mu_l(\tau) = \langle x_l \rangle_\pi$ , respectively. Thus, in practice, determining the fitting parameters involves computing the quantities  $C_{kl}$  and  $\mu_l$ , which together require evaluating  $2N + \frac{N(N-1)}{2}$  integrals over  $N$ -dimensional space, as well as inverting the covariance matrix  $C$ . Note that we have supposed that the exact potential leads to the condition  $C_{kk}^{-1}$  strictly positive for all  $k$ . This condition is expected to be verified for oscillators having a Hessian matrix at the equilibrium position with positive eigenvalues only.

Replacing in the expression of the discretized partition function, Eq.(14), the exact potential contribution by its gaussian approximation, Eq.(16), we get the following expression for  $Z_n$

$$Z_n(\beta) = \left( \frac{I}{I_G} \right)^n \left( \frac{1}{\sqrt{2\pi\tau}} \right)^{nN} \int \prod_{i=1}^n d\mathbf{x}^i e^{-\frac{1}{\tau} \sum_{i,j} \sum_{k=1}^N x_k^i A_{ij} x_k^j - \tau \sum_{i=1}^n V_G(\mathbf{x}^i)}. \quad (26)$$

The argument of the exponential being a quadratic form in the  $nN$  variables, the integral can be evaluated analytically. Let us outline the main steps of this calculation. Introducing the quantity  $\bar{x}_k$  defined as

$$\bar{x}_k \equiv -\frac{b_{gk}}{\omega_{gk}^2} \quad (27)$$

we have

$$Z_n = \left( \frac{I}{I_G} \right)^n \left( \frac{1}{\sqrt{2\pi\tau}} \right)^{nN} e^{\frac{\beta}{2} \sum_{k=1}^N \frac{b_{gk}^2}{\omega_{gk}^2}} \times \int \prod_{i=1}^n d\mathbf{x}^i e^{-\frac{1}{\tau} \sum_{i,j} \sum_{k=1}^N x_k^i A_{ij} x_k^j}$$

$$\times e^{-\tau \left[ \sum_{i=1}^n \sum_{k=1}^N \frac{1}{2} \omega_{gk}^2 x_k^{i2} + \sum_{1 \leq k < l \leq N} K_{gkl} (x_k^i + \bar{x}_k) (x_l^i + \bar{x}_l) \right]}.$$

Introducing the quantities  $\bar{K}_{gk}$  defined as

$$\bar{K}_{gk} \equiv \sum_{l=1}^N K_{gkl} \bar{x}_l \quad (28)$$

$Z_n$  becomes

$$Z_n = \left( \frac{I}{I_G} \right)^n \left( \frac{1}{\sqrt{2\pi\tau}} \right)^{nN} e^{\frac{1}{2}\beta A} \int d\mathbf{x} e^{-P(\mathbf{x}^1, \dots, \mathbf{x}^n)}$$

where the quantity  $A$  is given by

$$A = \sum_{k=1}^N \frac{b_{gk}^2}{\omega_{gk}^2} - 2 \sum_{1 \leq k < l \leq N} K_{gkl} \bar{x}_k \bar{x}_l \quad (29)$$

and  $P$  is a polynomial of order 2 expressed as

$$P(\mathbf{x}^1, \dots, \mathbf{x}^n) = \frac{1}{\tau} \sum_{i,j} \sum_{k=1}^N x_k^i A_{ij} x_k^j$$

$$+ \tau \sum_{i=1}^n \left( \sum_{k=1}^N \frac{1}{2} \omega_{gk}^2 x_k^{i2} + \sum_{k=1}^N \bar{K}_{gk} x_k^i + \sum_{1 \leq k < l \leq N} K_{gkl} x_k^i x_l^i \right).$$

Note that the quadratic form couples only the variables that share either a common time index  $i$  or a common space index  $k$ . As a result, the diagonalization of the quadratic form can be carried out independently over the time and space indices. The "time" rotation consists in diagonalizing the matrix  $A$ . The transformed variables are defined as  $\tilde{x}_k^i = \sum_{j=1}^n O^{ij} x_k^j$  where  $O^{ij}$  is the transformation matrix. The corresponding eigenvalues are given by

$$\lambda_i = 1 - \cos \frac{2\pi}{n} (i-1) \quad i = 1, n.$$

For each oscillator  $k$  and pair of oscillators  $(k, l)$ , we have

$$\sum_{i=1}^n x_k^{2i} = \sum_{i=1}^n \tilde{x}_k^{2i}$$

$$\sum_{i=1}^n x_k^i x_l^i = \sum_{i=1}^n \tilde{x}_k^i \tilde{x}_l^i,$$

and

$$\sum_{i=1}^n x_k^i = \sum_{i=1}^n \sum_{j=1}^n O^{ji} \tilde{x}_k^j$$

After some elementary manipulations, we get

$$Z_n = \left( \frac{I}{I_G} \right)^n \left( \frac{1}{\sqrt{2\pi\tau}} \right)^{nN} e^{\frac{\beta}{2} A} \int d\mathbf{x} e^{-\sum_{i=1}^n P_i}$$

with

$$P_i = \sum_{k=1}^N \left( \frac{1}{\tau} \lambda_i + \tau \frac{1}{2} \omega_{gk}^2 \right) x_k^{i2} + \sum_{1 \leq k < l \leq N} K_{gkl} x_k^i x_l^i + \sum_{k=1}^N c_k^i x_k^i,$$

where  $c_k^i$  is defined as

$$c_k^i = \tau \bar{K}_{gk} \sum_{j=1}^n O^{ij}.$$

For each time coordinate  $i$ , we now perform the "space" rotation. The matrix  $Q^i$  to diagonalize writes

$$Q^i = \frac{\lambda_i}{\tau} \mathbb{I} + \frac{\tau}{2} M$$

where  $\mathbb{I}$  is the identity matrix and  $M$  the symmetric matrix given by

$$M = \begin{bmatrix} \omega_{g1}^2 & K_{g12} & \cdots & K_{g1N} \\ K_{g12} & \omega_{g2}^2 & \cdots & K_{g2N} \\ \vdots & \vdots & \ddots & \vdots \\ K_{g1N} & K_{g2N} & \cdots & \omega_{gN}^2 \end{bmatrix} \quad (30)$$

In the absence of coupling, all eigenvalues of the matrix are positive. In physical applications where the coupling terms do not destabilize the system, this property remains valid. Accordingly, we assume throughout that all eigenvalues remain positive. Let  $\Omega_{gk}^2$  denote the eigenvalues of the  $M$  matrix and  $S_{kl}$  the corresponding transformation matrix. The transformed variables are expressed as

$$y_k^i = \sum_{l=1}^N S_{kl} x_l^i.$$

The eigenvalues of the matrix  $Q^i$  will be denoted as  $\nu_k^i$ ; they are given by

$$\nu_k^i = \frac{1}{\tau} \lambda_i + \frac{\tau}{2} \Omega_{gk}^2.$$

The diagonalization of the quadratic form,  $P^i$  leads to

$$P^i = \sum_{k=1}^N \nu_k^i y_k^{i2} + u_k^i y_k^i,$$

where  $u_k^i$  is defined as

$$u_k^i = \sum_{l=1}^N c_l^i (S^T)_{lk}.$$

After integrating out the variables  $y_k^i$ , we get

$$Z_n = \left( \frac{I}{I_G} \right)^n e^{\frac{\beta}{2} A} e^{-\sum_{i=1}^n \sum_{k=1}^N \frac{u_k^{i2}}{4\nu_k^i}} \prod_{i=1}^n \prod_{k=1}^N \frac{1}{\sqrt{2\tau\nu_k^i}}$$

In Appendix A the following relation is derived

$$\sum_{i=1}^n \frac{\left(\sum_j O^{ij}\right)^2}{\lambda_i + \tau^2 x} = \frac{n^2}{\beta \tau x}.$$

Using this equality, we can show that

$$\sum_{i=1}^n \sum_{k=1}^N \frac{u_k^{i2}}{4\nu_k^i} = \frac{\beta}{2} \sum_{k=1}^N \frac{(\sum_l \bar{K}_{gl} S_{lk}^T)^2}{\Omega_{gk}^2} \quad (31)$$

Now, using Eqs.(29) and (31), the partition function is written as

$$Z_n = \left(\frac{I}{I_G}\right)^n e^{\frac{\beta \mathcal{A}}{2}} \prod_{i=1}^n \prod_{k=1}^N \frac{1}{\sqrt{2\tau\nu_k^i}}$$

where the quantity  $\mathcal{A}$  is defined as

$$\mathcal{A} = \sum_{k=1}^N \frac{b_{gk}^2}{\omega_{gk}^2} - 2 \sum_{1 \leq k < l \leq N} K_{gkl} \bar{x}_k \bar{x}_l + \sum_{k=1}^N \frac{(\sum_l \bar{K}_{gl} S_{lk}^T)^2}{\Omega_{gk}^2}.$$

Quite remarkably, this expression can be rewritten in a more compact form. In Appendix A we show that

$$\mathcal{A} = (b_g, M^{-1} b_g) \quad (32)$$

where  $M$  is the matrix given in Eq.(30).  $I_G$  being a gaussian integral, it can be explicitly evaluated. It is given by

$$I_G = I_0 e^{\frac{\mathcal{A}}{2}} (b_g, M^{-1} b_g)$$

where

$$I_0 = \prod_{k=1}^N \sqrt{\frac{2\pi}{\tau \Omega_{gk}^2}}. \quad (33)$$

Finally, the discretized partition function given in Eq.(26) writes

$$Z_n = \left(\frac{I}{I_0}\right)^n \prod_{i=1}^n \prod_{k=1}^N \frac{1}{\sqrt{2\tau\nu_k^i}}. \quad (34)$$

Given the somewhat lengthy nature of the calculation, it may be worthwhile to verify the result numerically. This can be achieved by rewriting the original multidimensional integral, Eq. (26), in the form  $\int d\mathbf{x} e^{-\frac{1}{2}(\mathbf{x}, A\mathbf{x}) - B\mathbf{x}}$  where  $A$  is an  $nN \times nN$  matrix and  $B$  a vector of size  $nN$ . By numerically inverting the matrix  $A$ , one can then apply the standard result for Gaussian integrals

$$\int d\mathbf{x} e^{-\frac{1}{2}(\mathbf{x}, A\mathbf{x}) - B\mathbf{x}} = (\sqrt{2\pi})^{nN} \frac{1}{\sqrt{\det A}} e^{\frac{1}{2}(B, A^{-1} B)} \quad (35)$$

and verify numerically the equality between Eqs. (26) and (34).

The next step consists in performing the infinite- $n$  limit of the product,  $\prod_{i=1}^n \frac{1}{\sqrt{2\tau\nu_k^i}}$  in  $Z_n$ , Eq.(34). Using the following formula (see its derivation in appendix A of [18])

$$\lim_{n \rightarrow \infty} \prod_{i=1}^n \frac{1}{\sqrt{2\lambda_i + \frac{x^2}{n^2}}} = \frac{1}{e^{\frac{x}{2}} - e^{-\frac{x}{2}}}$$

we get

$$\lim_{n \rightarrow \infty} \prod_{i=1}^n \frac{1}{\sqrt{2\tau\nu_k^i}} = \frac{1}{e^{\frac{\beta\Omega_{gk}}{2}} - e^{-\frac{\beta\Omega_{gk}}{2}}}.$$

Finally, our partition function becomes

$$\mathcal{Z}_n = \mathcal{N}_n \prod_{k=1}^N \frac{1}{e^{\frac{\beta\Omega_{gk}}{2}} - e^{-\frac{\beta\Omega_{gk}}{2}}} \quad (36)$$

where the prefactor  $\mathcal{N}_n$  can take two possible equivalent expressions

$$\mathcal{N}_n = \left(\frac{I}{I_0}\right)^n \quad (37)$$

or

$$\mathcal{N}_n = \left(\frac{I}{I_G}\right)^n e^{\frac{\mathcal{A}}{2}}. \quad (38)$$

Note that both expressions will be used in the following.

Taking the limit  $n \rightarrow \infty$  in the partition function  $\mathcal{Z}_n$  is not possible since the prefactor  $\mathcal{N}_n$  does not converge to a finite value -except in the special case of a harmonic potential where  $I = I_0$ . At this point, we introduce the second key idea of this work. Following what we have done in the one-dimensional case,[18, 19], we propose not to take this limit but, instead, to evaluate the partition function at a *finite* value of  $n$  or time step  $\tau$ . As in the 1d-case, we invoke a Principle of Minimal Sensitivity (PMS) which imposes the partition function to be the least sensitive to the variations of the fitting parameters introduced in the Gaussian approximation. However, as we shall see now, because of the too many constraints resulting from the PMS constraints, using only a single value of  $n$  is no longer possible here in the multi-dimensional case. Let us now make this more precise. For each index  $k$  and each pair  $(k, l)$ , we require the following PMS conditions to be satisfied

$$\frac{\partial \mathcal{Z}_n}{\partial \omega_{gk}(\tau)} = 0, \quad (39)$$

$$\frac{\partial \mathcal{Z}_n}{\partial K_{gkl}(\tau)} = 0. \quad (40)$$

Note that the condition  $\frac{\partial \mathcal{Z}_n}{\partial b_{gk}(\tau)} = 0$  is not considered, as it is automatically satisfied due to the independence of  $\mathcal{Z}_n$  from the vector  $\mathbf{b}_g$ ; see Eqs. (36) and (37).

In the one-dimensional case,[18, 19] there is only one fitting parameters  $\omega_g$  and the PMS condition reduces to

$$\frac{\partial \mathcal{Z}_n}{\partial \omega_g(\tau)} = 0. \quad (41)$$

This condition leads to the following equation for the variable  $\tau$

$$\tau = \frac{2}{\omega_g(\tau) \coth \frac{\beta \omega_g(\tau)}{2}} \quad (42)$$

where the effective frequency,  $\omega_g(\tau)$  is given by

$$\omega_g(\tau) = \frac{1}{\sqrt{\tau \langle (x - \langle x \rangle)^2 \rangle}}, \quad (43)$$

see Eq.(23). For the quartic oscillator, we have shown[18] that the nonlinear PMS equation, Eq. (42), admits a unique solution,  $\tau_c(\beta)$ .

In the general multi-dimensional case, the PMS conditions can be reformulated as

$$\tau = \frac{2 \sum_{k=1}^N \frac{\partial \Omega_{gk}(\tau)}{\partial p} \frac{1}{\Omega_{gk}(\tau)}}{\sum_{k=1}^N \frac{\partial \Omega_{gk}(\tau)}{\partial p} \coth \frac{\beta \Omega_{gk}(\tau)}{2}} \quad (44)$$

where  $p$  denotes one of the fitting parameters in the set  $\{\omega_{gk}(\tau), K_{gkl}(\tau)\}$ . This system of  $M = N + \frac{N(N-1)}{2}$  equations [combined with the expressions Eqs.(23),(24), and (25) for the fitting parameters] is overdetermined and no solution in  $\tau$  can be found in general. To proceed, let us first consider the case of a system of  $N$  *uncoupled* quantum oscillators. In this case, the covariance matrix,  $\langle (x - \langle x_k \rangle)(x - \langle x_l \rangle) \rangle$  is diagonal, the fitting parameters  $K_{gkl}$  vanish (see, Eq.(24)), and the partition function factorizes under the form

$$\mathcal{Z}_n = \prod_{k=1}^N z_n^k \quad (45)$$

where the  $z_n^k$ 's are the partition functions of  $N$  independent one-dimensional oscillators with effective frequency  $\omega_{gk}(\tau)$ . The PMS equations to be solved are now decoupled into  $N$  one-dimensional PMS equations, leading to  $N$  *different* time-steps,  $\tau_k(\beta)$ . In presence of couplings the generalization is therefore rather natural: A time-step per fitting parameter is introduced and the PMS equations become a system of  $M = N + \frac{N(N-1)}{2}$  equations with  $M$  unknowns, a system that may now admit a solution. Denoting  $\tau_k$  and  $\tau_{kl}$  the unknown time-steps associated with  $\omega_{gk}$  and  $K_{gkl}$ , respectively, the new PMS equations write

$$\tau_k = \frac{2 \sum_{i=1}^N \frac{\partial \Omega_{gi}([\tau])}{\partial \omega_{gk}} \frac{1}{\Omega_{gi}([\tau])}}{\sum_{i=1}^N \frac{\partial \Omega_{gi}([\tau])}{\partial \omega_{gk}} \coth \frac{\beta \Omega_{gi}([\tau])}{2}}. \quad (46)$$

and

$$\tau_{kl} = \frac{2 \sum_{i=1}^N \frac{\partial \Omega_{gi}([\tau])}{\partial K_{gkl}} \frac{1}{\Omega_{gi}([\tau])}}{\sum_{i=1}^N \frac{\partial \Omega_{gi}([\tau])}{\partial K_{gkl}} \coth \frac{\beta \Omega_{gi}([\tau])}{2}}. \quad (47)$$

Here,  $[\tau]$  denotes the complete set of time-steps, that is,  $[\tau] = (\tau_1, \dots, \tau_N, \tau_{12}, \dots, \tau_{N-1,N})$ . The existence of a solution to the PMS equations -a system of coupled, nonlinear equations- is a highly nontrivial mathematical problem. Moreover, multiple solutions may exist. In the numerical simulations presented below, which involve simple systems with up to ten coupled oscillators, we employed a simple iterative procedure to solve these equations. When initialized with reasonable estimates for the time-steps, this method systematically converged. However, such convergence cannot be guaranteed for all types of potentials or larger numbers of oscillators. A more detailed investigation of this important but challenging issue is left for future work. Having introduced multiple time-steps, the distribution  $\pi$  associated with  $e^{-\tau V}$  needs to be generalized. Using Eq.(12) for the potential, the multiple time-step distribution writes

$$\pi = \frac{e^{-\sum_{k=1}^N \tau_k V_k(x_k) - \sum_{1 \leq k < l \leq N} \tau_{kl} V_{kl}}}{\int d\mathbf{x} e^{-\sum_{k=1}^N \tau_k V_k(x_k) - \sum_{1 \leq k < l \leq N} \tau_{kl} V_{kl}}}. \quad (48)$$

The conditions determining the fitting parameters, Eqs.(17) and (18), must also be generalized. The new fitting parameters are now given by

$$\omega_{gk}([\tau]) = \sqrt{\frac{C_{kk}^{-1}([\tau])}{\tau_k}} \quad (49)$$

$$K_{gkl}([\tau]) = \frac{C^{-1}([\tau])_{kl}}{\tau_{kl}} \quad (50)$$

and

$$b_{gk}([\tau]) = -\frac{(C^{-1}([\tau])\mu)_k}{\tau_k} \quad (51)$$

where the covariance matrix  $C$  and the vector of first-order moments  $\mu$  are calculated using the multiple time-step distribution  $\pi$ , Eq.(48). Note that, in the high-temperature regime,  $\beta \rightarrow 0$ ,  $n \sim 1$ , and all time-steps become identical with  $\tau \sim \beta$ , see Eqs.(46) and (47). Using Eqs.(36) and (37) for the PF, we get

$$\mathcal{Z} \rightarrow \frac{I}{I_0} \prod_{k=1}^N \frac{1}{\beta \Omega_{gk}} \quad (52)$$

and using expression (33) for  $I_0$

$$\mathcal{Z} \rightarrow \left( \frac{1}{\sqrt{2\pi\beta}} \right)^N \int d\mathbf{x} e^{-\beta V(\mathbf{x})}, \quad (53)$$

which is the exact classical limit. At finite temperature, the time steps generally differ, and the prefactor  $\mathcal{N}_n$  of

$\mathcal{Z}_n$  becomes ill-defined due to the ambiguity in choosing  $n$  (or equivalently,  $\tau$ ). An additional prescription is thus required to determine the prefactor. A first possibility could be to define a *single* effective time step, for instance, as a weighted average of the individual time steps  $\tau_k$ 's, *i.e.*,  $\bar{\tau} = \sum_k w_k \tau_k$ . At small  $\beta$  where all  $\tau_k$  values become close, this approximation makes sense, as the classical limit is recovered. However, at large  $\beta$  numerical results indicate that this approximation deteriorates significantly. After some experimentation, we found that a more robust and accurate strategy is to approximate the prefactor by neglecting the coupling terms in the multi-dimensional integrals  $I$  and  $I_G$ . To implement this idea the form (38) for the prefactor is more adapted than (37). The approximation we propose here writes as follows

$$\mathcal{N}_n = \left( \frac{I}{I_G} \right)^n e^{\frac{\beta}{2}\mathcal{A}} \simeq \prod_{k=1}^N \left( \frac{I_k(\tau_k)}{I_{Gk}([\tau])} \right)^{\frac{\beta}{\tau_k}} e^{\frac{\beta}{2}\mathcal{A}([\tau])} \quad (54)$$

where

$$I_k(\tau_k) = \int dx_k e^{-\tau_k V_k(x_k)} \quad (55)$$

and

$$I_{Gk}([\tau]) = \int dx_k e^{-\tau_k (\frac{1}{2}\omega_{gk}^2([\tau])x_k^2 + b_{gk}([\tau])x_k)}. \quad (56)$$

Note that the  $K_{gkl}$ 's are zeroed only in the multi-dimensional integrals  $I$  and  $I_G$  and not in  $\mathcal{A}$  which is exactly evaluated. Note also that with such a choice the classical limit is no longer exactly recovered. However, numerical simulations show that the corresponding error is small.

To summarize let us present a schematic algorithm for the evaluation of the partition function:

i) Start with some initial values for the time-steps,  $[\tau] = (\tau_1, \dots, \tau_N, \tau_{12}, \dots, \tau_{N-1N})$ .

ii) Evaluate numerically the vector of first-order moments,  $\mu_k = \langle x_k \rangle_\pi$ , and the covariance matrix  $C_{kl} = \langle (x_k - \mu_k)(x_l - \mu_l) \rangle_\pi$  with the multiple-step distribution  $\pi$ , Eq.(48).

iii) Evaluate numerically the inverse of the covariance matrix.

iv) Evaluate the new fitting parameters,  $\omega_{gk}([\tau])$ ,  $b_{gk}([\tau])$ , for  $k = 1$  to  $N$  and  $K_{gkl}([\tau])$  for  $k, l = 1$  to  $N$  with  $k < l$  using Eqs.(49),(50), and (51).

v) Evaluate the new time-steps using the PMS equations, Eqs.(46,47), where the frequencies  $\Omega_{gk}$  are obtained by diagonalizing the matrix  $M_{kl} = \omega_{gk}([\tau])\delta_{kl} + K_{gkl}([\tau])$ , Eq.(30). In practice, the derivatives of the eigenvalues  $\Omega_{gk}$ 's with respect to the fitting parameters can be

conveniently performed using a finite-difference scheme.

vi) Go to step ii) and iterate up to convergence of the time-steps.

vii) Finally, evaluate the partition function using Eqs.(36),(54),(55), and (56).

### III. NUMERICAL APPLICATIONS

#### A. Quantum oscillators for $N=1,2$ , and 3. Comparison with exact numerical results

In this section, we consider systems consisting of  $N = 1, 2$ , and 3 coupled anharmonic oscillators and compare our results with "exact" numerical calculations. These reference values are obtained by diagonalizing the Hamiltonian matrix in a sufficiently large Gaussian basis set to ensure convergence of the energy levels. The partition function is then computed as a sum over a sufficiently large number of components,  $e^{-\beta E_i}$ . We present numerical results for the free energy,  $F = -\frac{1}{\beta} \log Z$ , the average energy,  $E = -\frac{\partial \log Z}{\partial \beta}$ , and the specific heat,  $c_v = \frac{\partial E}{\partial \beta}$ .

The results are illustrated for a Hamiltonian with a potential of quartic polynomial form

$$H = -\frac{1}{2} \sum_{k=1}^N \frac{\partial^2}{\partial x_k^2} + \sum_{k=1}^N \frac{1}{2} \omega_k^2 x_k^2 + \lambda \left( \sum_{k=1}^N \mu_k x_k^3 + g_k x_k^4 + \sum_{1 \leq k < l \leq N} V_{kl} \right) \quad (57)$$

where the coupling term is written as

$$V_{kl} = c_{kl}^{(1)} x_k x_l + c_{kl}^{(2)} x_k^2 x_l + c_{lk}^{(2)} x_l^2 x_k + c_{kl}^{(3)} x_k^2 x_l^2 \quad (58)$$

Here, the parameter  $\lambda$  is introduced to study the impact of both anharmonicity and coupling strength on the results. In the following applications, the parameters are chosen as follows

$$\omega_k = 1 + 0.2(k-1)$$

$$\mu_k = -0.25 + 0.3(k-1)$$

$$g_k = 1 + 0.1(k-1)$$

$$c_{kl}^{(1)} = 0.5 \quad c_{kl}^{(2)} = 0.2 \quad c_{lk}^{(2)} = 0.1 \quad c_{kl}^{(3)} = 0.1 \quad \text{for } k < l.$$

Note that we have chosen  $c_{kl}^{(2)} \neq c_{lk}^{(2)}$  to consider the general case of a non-symmetric coupling matrix  $V_{kl}$ . Calculating the average energy and specific heat requires

evaluating the first and second derivatives of the partition function with respect to the inverse temperature  $\beta$ . While it is, in principle, possible to derive explicit analytical expressions for these derivatives, the resulting formulas tend to be quite involved. This complexity arises primarily from the need to differentiate the eigenvalues  $\Omega_k$ . In practice, a more simple and computationally efficient approach is to approximate the derivatives using finite-difference methods. We use the following formulas

$$E = -\frac{\log Z(\beta + \epsilon) - \log Z(\beta - \epsilon)}{2\epsilon}$$

and

$$c_v = \beta^2 \frac{\log Z(\beta + \epsilon) - 2\log Z(\beta) + \log Z(\beta - \epsilon)}{\epsilon^2}$$

where  $\epsilon$  denotes a small variation in  $\beta$ . In practice, we have observed that the computed quantities stabilize rapidly as  $\epsilon$  is decreased, confirming that the finite-difference approach proposed here is appropriate. From a numerical point of view, the most computationally demanding step is the evaluation, at each iteration of the algorithm, of the  $M = N + \frac{N(N+1)}{2}$  integrals of dimension  $N$  corresponding to the components of the first-order moment vector and of the covariance matrix. For the small number of oscillators considered in this section, we found that using a simple Riemann integration scheme with a sufficiently fine uniform grid is sufficient. The case of much larger  $N$  will be addressed in the next section.

Tables I, II, and III present a comparison between the results obtained using our approximate partition function and exact numerical results for systems of one, two, and three oscillators, respectively. Each table reports the free energy, average energy, and specific heat -each expressed per oscillator. Results are provided for three selected inverse temperatures,  $\beta = 0.5, 1.$  and  $2.$ , and for three values of the anharmonicity/coupling parameter  $\lambda = 0.1, 1,$  and  $2.$  At the smallest inverse temperature considered (*i.e.*, highest temperature),  $\beta = 0.4,$  and for the weakest anharmonicity and coupling,  $\lambda = 0.1,$  the relative errors for all quantities are particularly small -typically less than 1%, with a maximum of 1.5% for  $N = 3.$  This high-level of accuracy is not surprising since our approximate partition function becomes exact in the limit  $\lambda \rightarrow 0$  and is also nearly exact as  $\beta \rightarrow 0$  (Recall that, for  $N \geq 2,$  there is a small error left due to the approximation of the ratio of integrals, Eq. 54). As the temperature decreases, the relative errors increase slightly but remain small -typically within a few percent. Note that the errors in the various quantities at  $\beta = 1$  and  $\beta = 2$  are similar, and this trend persists for larger values of  $\beta$  (not shown), indicating no degradation of accuracy at lower temperatures. As expected, the errors increase with stronger anharmonicity and coupling, but they remain modest, again within a few percent. A slight increase in error is also observed as the number of oscillators increases; however, given the small system sizes considered here, it is difficult to draw a firm conclusion regarding a general

trend. This point will be further explored in the next section, where larger systems are investigated. Overall, we conclude that for the small systems considered in this section, the model yields quite accurate results over a broad range of parameters.

## B. Quantum oscillators for $N > 3.$ Comparison with PIMC

In this section, we study the applicability and precision of our approximate formula for systems with larger numbers of oscillators. To this end, we consider a system of  $N$  coupled quartic oscillators described by the Hamiltonian

$$H = -\frac{1}{2} \sum_{k=1}^N \frac{\partial^2}{\partial x_k^2} + \sum_{k=1}^N \frac{1}{2} \omega^2 x_k^2 + g x_k^4 + K \sum_{k=1}^N x_k x_{k+1} \quad (59)$$

with  $x_{N+1} = x_N$  (periodic conditions). Physically, this Hamiltonian can describe, for instance, a chain of coupled oscillators in solid-state physics,[28] or it may arise from the discretization of a quantum field theory, such as the  $\phi^4$ -theory.[29] In the applications to follow, the Hamiltonian parameters are fixed as  $\omega = 1,$   $g = 1,$  and  $K = 0.8.$  As already mentioned, when the number of oscillators becomes large, it becomes increasingly difficult to obtain "exact" thermodynamic quantities from numerical diagonalization. To assess the accuracy of our analytical approximation for large systems, we thus compare our results to data obtained with Path Integral Monte Carlo (PIMC).

Thanks to the symmetry of the Hamiltonian (translational symmetry and oscillators with identical frequency  $\omega$  and coupling constant  $g$ ) the first-order moments vanish and the covariance matrix  $C_{kl}$  depends only on the distance,  $d(k, l),$  between  $k$  and  $l$  on the circle of length  $N,$  that is

$$C_{kl} = \mathcal{C}[d(k, l)] \quad (60)$$

where  $d(k, l)$  is given by

$$d(k, l) = \text{Min}(|k - l|, N - |k - l|), \quad (61)$$

and  $\mathcal{C}$  is some function to determine. Mathematically, it means that the covariance matrix is a symmetric circulant matrix.[30] Here, we shall write it under the following form

$$C = \begin{bmatrix} C_{[0]} & C_{[1]} & \cdots & C_{[2]} & C_{[1]} \\ C_{[1]} & C_{[0]} & C_{[1]} & & C_{[2]} \\ \vdots & C_{[1]} & C_{[0]} & \ddots & \vdots \\ C_{[2]} & & \ddots & \ddots & C_{[1]} \\ C_{[1]} & C_{[2]} & \cdots & C_{[1]} & C_{[0]} \end{bmatrix}, \quad (62)$$

with the notation

$$C_{[m]} \equiv \mathcal{C}[d(k, l) = m], \quad (63)$$

Table I.  $N = 1$ . Numerical comparison between approximate and exact thermodynamic quantities  $F/N, E/N$ , and  $c_v/N$  for three values of the inverse temperature  $\beta$  and  $\lambda$ . Relative errors  $\epsilon$  (in %) on each quantity  $Q$  is reported,  $\epsilon = (Q_{model} - Q_{ex})/Q_{ex} \times 100$ .

	$\beta = 0.5$			$\beta = 1$			$\beta = 2$		
	Approximate	Exact	$\epsilon(\%)$	Approximate	Exact	$\epsilon(\%)$	Approximate	Exact	$\epsilon(\%)$
$\lambda = 0.1$									
$F/N$	-0.88533	-0.88174	0.4	0.22177	0.22530	-1.5	0.51023	0.51336	-0.6
$E/N$	1.82260	1.82620	-0.1	1.02293	1.02605	-0.3	0.66944	0.67188	-0.3
$c_v/N$	0.81039	0.81051	-0.01	0.77154	0.77275	-0.1	0.58292	0.58383	-0.1
$\lambda = 1$									
$F/N$	-0.07155	-0.05308	34.7 <sup>a</sup>	0.63108	0.65114	-3.0	0.76903	0.78853	-2.4
$E/N$	1.76696	1.78923	-1.2	1.07432	1.09472	-1.8	0.82153	0.83995	-2.1
$c_v/N$	0.72839	0.72810	0.04	0.62244	0.62754	-0.8	0.31544	0.31443	0.3
$\lambda = 2$									
$F/N$	0.24716	0.27430	-9.8	0.81631	0.84537	-3.4	0.90999	0.93837	-3.0
$E/N$	1.79690	1.82933	-1.7	1.14493	1.17396	-2.4	0.93770	0.96524	-2.8
$c_v/N$	0.70239	0.70277	-0.05	0.55615	0.56267	-1.1	0.20823	0.20523	1.4

<sup>a</sup>The relative error is accidentally large because  $F/N$  is small. This is not the case of the absolute error.

Table II.  $N = 2$  Numerical comparison between approximate and exact thermodynamic quantities  $F/N, E/N$ , and  $c_v/N$  for three values of the inverse temperature  $\beta$  and  $\lambda$ . Relative errors  $\epsilon$  (in %) on each quantity  $Q$  is reported,  $\epsilon = (Q_{model} - Q_{ex})/Q_{ex} \times 100$ .

	$\beta = 0.5$			$\beta = 1$			$\beta = 2$		
	Approximate	Exact	$\epsilon(\%)$	Approximate	Exact	$\epsilon(\%)$	Approximate	Exact	$\epsilon(\%)$
$\lambda = 0.1$									
$F/N$	-0.76924	-0.76164	0.9	0.29453	0.29941	-1.6	0.56197	0.56555	-0.6
$E/N$	1.85611	1.85777	-0.08	1.05101	1.05325	-0.2	0.70362	0.70596	-0.3
$c_v/N$	0.81893	0.81813	0.09	0.77034	0.77025	0.01	0.55403	0.55308	0.1
$\lambda = 1$									
$F/N$	-0.0052	0.00209	-125.2 <sup>a</sup>	0.67649	0.70023	-3.3	0.80700	0.82876	-2.6
$E/N$	1.79059	1.81194	-1.1	1.10069	1.12119	-1.8	0.85541	0.87524	-2.2
$c_v/N$	0.72907	0.72816	0.1	0.61345	0.61672	-0.5	0.29649	0.292335451	1.4
$\lambda = 2$									
$F/N$	0.30146	0.33755	-10.6	0.85463	0.88860	-3.8	0.94452	0.97632	-3.2
$E/N$	1.81591	1.84862	-1.7	1.17084	1.20121	-2.5	0.97127	1.00130	-2.9
$c_v/N$	0.69994	0.69953	0.05	0.54242	0.54748	-0.9	0.19784	0.19119	3.4

<sup>a</sup>The relative error is accidentally large because  $F/N$  is small. This is not the case of the absolute error.

where the distance  $m$  varies from  $m = 0$  to  $\lfloor \frac{N}{2} \rfloor$ ,  $\lfloor \frac{N}{2} \rfloor$  denoting the euclidean division. This notation will be used for all symmetric circulant matrices to follow. Due to i) the structure of the PMS equations, Eqs.(46,47), ii) the relations giving the fitting parameters, Eqs.(49,50,51) and iii) the fact that the inverse of a symmetric circulant matrix is a symmetric circulant matrix, we have the following properties:

- i) The  $\omega_{gk}$ 's and  $\tau_k$ 's are independent of  $k$
- ii) The matrices  $K_{gkl}$ ,  $M_{kl}$ , and  $\tau_{kl}$  are all three symmetric circulant matrices.

Finally, let us note that the spectrum of a circulant matrix is analytically known. For the matrix  $M$  the eigenvalues  $\Omega_{gi}$  are as follows.

For  $N$  even

$$\Omega_{gi} = \sqrt{\omega_g^2 + K_{\lfloor \frac{N}{2} \rfloor} (-1)^i + 2 \sum_{j=1}^{\frac{N}{2}-1} K_{[j]} \cos\left(\frac{2\pi}{N} ji\right)} \quad i = 1, N. \quad (64)$$

For  $N$  odd

$$\Omega_{gi} = \sqrt{\omega_g^2 + 2 \sum_{j=1}^{\frac{N-1}{2}} K_{[j]} \cos\left(\frac{2\pi}{N} ji\right)} \quad i = 1, N. \quad (65)$$

where

$$\omega_g = \sqrt{\frac{C_{[0]}^{-1}}{\tau_{[0]}}} \quad (66)$$

Table III.  $N = 3$ . Numerical comparison between approximate and exact thermodynamic quantities  $F/N, E/N$ , and  $c_v/N$  for three values of the inverse temperature  $\beta$  and  $\lambda$ . Relative errors  $\epsilon$  (in %) on each quantity  $Q$  is reported,  $\epsilon = (Q_{model} - Q_{ex})/Q_{ex} \times 100$ .

	$\beta = 0.5$			$\beta = 1$			$\beta = 2$		
	Approximate	Exact	$\epsilon(\%)$	Approximate	Exact	$\epsilon(\%)$	Approximate	Exact	$\epsilon(\%)$
$\lambda = 0.1$									
$F/N$	-0.65609	-0.64610	1.5	0.36535	0.37092	-1.5	0.61321	0.61701	-0.6
$E/N$	1.88765	1.88758	0.03	1.07902	1.08066	-0.1	0.73936	0.74169	-0.3
$c_v/N$	0.82630	0.82386	0.2	0.76617	0.76501	0.1	0.52290	0.52076	0.4
$\lambda = 1$									
$F/N$	0.05707	0.08642	-33.9 <sup>a</sup>	0.71980	0.74432	-3.2	0.84354	0.86540	-2.5
$E/N$	1.81391	1.83301	-1.0	1.12669	1.14606	-1.6	0.88818	0.90779	-2.1
$c_v/N$	0.72951	0.72743	0.2	0.60509	0.60693	-0.3	0.27975	0.27380	2.1
$\lambda = 2$									
$F/N$	0.34997	0.38834	-9.8	0.88935	0.92355	-3.7	0.97555	1.00700	-3.1
$E/N$	1.83413	1.86428	-1.6	1.19456	1.22352	-2.3	1.00085	1.03027	-2.8
$c_v/N$	0.69776	0.69575	0.2	0.53199	0.53592	-0.7	0.18852	0.18026	4.5

<sup>a</sup>)The relative error is accidentally large because  $F/N$  is small. This is not the case of the absolute error.

and

$$K_{[m]} = \frac{C_{[m]}^{-1}}{\tau_{[m]}} \quad m = 1, \lfloor \frac{N}{2} \rfloor \quad (67)$$

In these relations,  $\tau_{[0]} = \tau_k$  and  $\tau_{[m]} = \tau_{kl}$ .

Finally, the PMS equations to solve write in the form

$$\tau_{[m]} = \frac{2 \sum_{i=1}^N \cos\left(\frac{2\pi}{N} mi\right) \frac{1}{\Omega_{gi}^2}}{\sum_{i=1}^N \cos\left(\frac{2\pi}{N} mi\right) \frac{1}{\Omega_{gi}} \coth \frac{\beta \Omega_{gi}}{2}} \quad m = 0, \lfloor \frac{N}{2} \rfloor \quad (68)$$

As already remarked, the main computational burden

is the evaluation of the covariance matrix written here as

$$C_{kl} = \frac{\int dx x_k x_l e^{-\tau_{[0]} \sum_{i=1}^N V_i(x_i) - \tau_{[1]} K \sum_{i=1}^N x_i x_{i+1}}}{\int dx e^{-\tau_{[0]} \sum_{i=1}^N V_i(x_i) - \tau_{[1]} K \sum_{i=1}^N x_i x_{i+1}}} \quad (69)$$

For that, we shall resort to a deterministic approach based on a systematic expansion of the interacting part of the potential

$$e^{-\tau_{[1]} K \sum_{i=1}^N x_i x_{i+1}} = \sum_{p=0}^{\infty} \frac{(-\tau_{[1]} K)^p}{p!} \left( \sum_{i=1}^N x_i x_{i+1} \right)^p \quad (70)$$

Using the formula

$$\left( \sum_{i=1}^N x_i x_{i+1} \right)^p = \sum_{k_1 + \dots + k_N = p} \frac{p!}{k_1! \dots k_N!} \prod_{i=1}^N x_i^{k_i + k_{i+1}} \quad (71)$$

with  $x_{N+1} = x_1$  and  $k_{N+1} = k_1$ , we get

$$C_{kl} = \frac{\sum_{p=0}^{\infty} (-K \tau_{[1]})^p \sum_{k_1 + \dots + k_N = p} \frac{1}{k_1! \dots k_N!} \prod_{i=1}^N J_{k_i + k_{i+1} + \delta_{ik} + \delta_{il}}(\tau_{[1]}, V_i)}{\sum_{p=0}^{\infty} (-K \tau_{[1]})^p \sum_{k_1 + \dots + k_N = p} \frac{1}{k_1! \dots k_N!} \prod_{i=1}^N J_{k_i + k_{i+1}}(\tau_{[1]}, V_i)} \quad (72)$$

where we have introduced the following one-dimensional integrals

$$J_n(\tau_{[1]}, V_i) = \int dx e^{-\tau_{[1]} V_i(x)} x^n \quad (73)$$

The number of partitions of the integer  $p$  grows exponentially, making this approach feasible only for a relatively small number of oscillators. In practice, the convergence of the sums as a function of  $p$  can be achieved

with sufficient accuracy for values up to approximately  $N \sim 10$ . To accelerate the convergence of the partial sums we have used here a Shank's transform.[31] For larger systems, deterministic computations become impractical, and stochastic methods must be considered. However, care must be taken due to the potentially severe impact of statistical noise on the iterative scheme. To circumvent this issue, a possibility is to introduce a correlated sampling strategy, that is, to use a fixed set of

configurations and to introduce some reweighting in the stochastic averages. We have implemented such a Monte Carlo approach and verified that it may work for larger values of  $N$ . However, we have observed that the stability of the iterative algorithm, in its simplest form, is no longer systematically maintained. This problem calls for further refinement and the development of more robust algorithms. A detailed investigation of these improvements is beyond the scope of the present work and is deferred to future research.

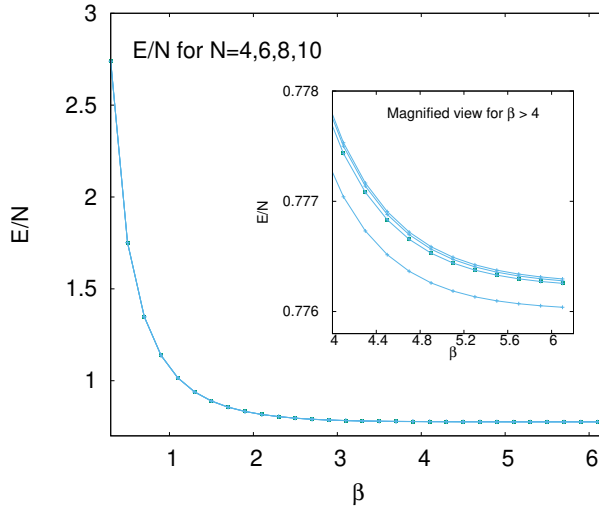


Figure 1. Average energy per oscillator  $E/N$  as a function of  $\beta$  for  $N = 4, 6, 8,$  and  $10$ . At the scale of the main figure, the curves for different  $N$  almost coincide. The inset shows a magnified view of the curves for  $\beta > 4$ . The lowest curve of the inset is that for  $N = 4$ .

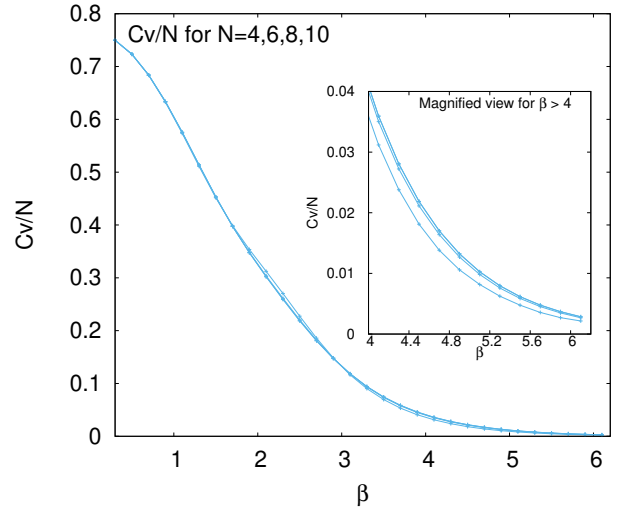


Figure 2. Specific heat per oscillator  $c_v/N$  as a function of  $\beta$  for  $N = 4, 6, 8,$  and  $10$ . At the scale of the main figure, the curves for different  $N$  almost coincide. The inset shows a magnified view of the curves for  $\beta > 4$ . The lowest curve of the inset is that for  $N = 4$ .

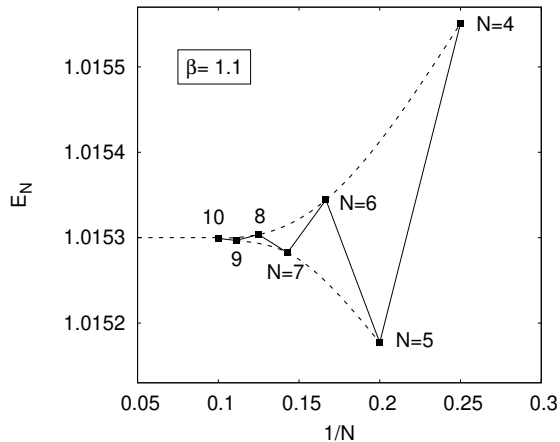


Figure 3.  $N$ -dependence of the average energy per oscillator  $E/N$  as a function of  $N$  for  $\beta = 1.1$ . For both  $N$  even and odd, a dashed line is drawn for guiding the eye.

In figure 1 and 2 we show the average energy and specific heat per oscillator as a function of  $\beta$  obtained with our approximate formula. Four curves corresponding to  $N = 4, 6, 8$  and  $10$  are depicted. As seen from the figures, the various curves almost coincide at the scale of the main figure, meaning that the finite-size effects are small. To have a closer look at these effects, an inset giving a magnified view of the curves at low temperatures,  $\beta > 4$ , is given for both figures. To solve the PMS equations, Eq.(68), we use a simple iterative process in which the different time-steps are evolved as follows

$$\tau_{[m]}^{n+1} = f_m(\tau_{[1]}^n, \tau_{[2]}^n, \dots) \quad (74)$$

where the superscript  $n$  is the iteration index and  $f_m$  is given by the R.H.S. of Eq.(68).

For all  $\beta$  and number of oscillators considered here ( $N \leq 10$ ) we have found that the iterative process is remarkably stable and converges rapidly in a few iterations to a unique set of time-steps, provided reasonable starting values,  $\tau_{[m]}^0$ , are chosen. In addition, both thermodynamic quantities are found to display a regular behavior when varying  $\beta$  and  $N$ , a satisfactory result for our approximate formula. In figure 3 we provide a quantitative

assessment of  $N$ -dependence of the average energy as a function of the number  $N$  of oscillators. The results are shown for a particular value of the inverse temperature,  $\beta = 1.1$ , but similar behaviors are obtained for all temperatures and for the specific heat too. As seen on the figure, a parity effect is observed as a function of  $N$ . However, both energy curves corresponding to  $N$  even and odd converge rapidly and smoothly to a common value for  $N = \infty$ .

To assess the accuracy of our approximate formula, we compare our results with "exact" numerical data obtained using Path Integral Monte Carlo (PIMC) simulations. Path integral methods are, in principle, numerically exact -provided the two primary sources of error are properly controlled. The first source of error is the systematic bias associated with using a finite number of time slices, or Trotter number,  $n$ . In practice, simulations are carried out for several values of  $n$ , and results are extrapolated to the limit  $n \rightarrow \infty$ . At high temperatures, the PIMC time step,  $\tau = \frac{\beta}{n}$ , can be made sufficiently small with moderate values of  $n$ , making the extrapolation relatively straightforward. However, at low temperatures, larger values of  $n$  are required, leading to more computationally intensive simulations. In addition to the systematic bias, one must account for statistical errors inherent to any stochastic (Monte Carlo) method. For each value of  $n$ , the statistical uncertainty must be reduced enough to enable a reliable extrapolation of thermodynamic properties to  $n \rightarrow \infty$ . Various PIMC implementations exist in the literature, each with different strengths in terms of efficiency and accuracy. However, our objective here is not to employ the most advanced algorithm, but rather to evaluate the accuracy of our approximate formula. To this end, we have implemented a standard PIMC approach based on Fourier modes and low-variance estimators for both the average energy and specific heat. The relevant expressions are detailed in Appendix B. To ensure a meaningful comparison with our approximate formula, the PIMC simulations were run long enough so that statistical errors are negligible on the scale of our figures. As is well known, the finite- $n$  bias becomes more pronounced as temperature decreases.[32] Here, this effect is particularly significant in the specific heat at low temperatures (see Figure 5). More sophisticated path-integral techniques -such as Path Integral Molecular Dynamics (PIMD) with optimized thermostats[32, 33]- could significantly reduce this bias. However, as already noted, such refinements are not critical here for our purpose.

Figures 4 and 5 display the average energy and specific heat per oscillator, respectively, as functions of  $\beta$  for  $N = 10$ . The PIMC results for  $n = 30, 40, 60$ , and  $80$  are shown together with the curves obtained using our approximate formula for comparison. Error bars on the PIMC data are smaller than the symbol size and are therefore not visible. For the average energy, the finite- $n$  biases are relatively small for all temperatures at the scale of the figure, and our approximate curve

closely follows the PIMC results. A magnified view of the curves is provided in the inset, where we focus on the low-temperature regime ( $\beta > 3.5$ ), where the approximation error of our formula is expected to be maximal. The PIMC results for various  $n$  values have been extrapolated to  $n \rightarrow \infty$  using a quadratic fit. Notably, individual PIMC curves at finite  $n$  do not exhibit the expected saturation behavior as the temperature goes to zero and have, instead, a spurious linear decreasing behavior. Only, the extrapolated curve displays this correct asymptotic behavior. Remarkably, our approximate expression for the average energy captures this saturation and remains remarkably parallel to the extrapolated exact PIMC curve over the entire temperature range. For the specific heat, a stronger dependence on the Trotter number  $n$  is observed at low temperatures. As for the average energy, extrapolation yields a meaningful "exact" numerical curve that correctly converges to zero at low temperatures. At finite  $n$ , The PIMC curves display an unphysical minimum and increase indefinitely at small temperatures. As expected from the fact that the error in the approximate energy curve was nearly independent of the temperature, a remarkably accurate approximate curve for the specific heat is obtained with our formula.

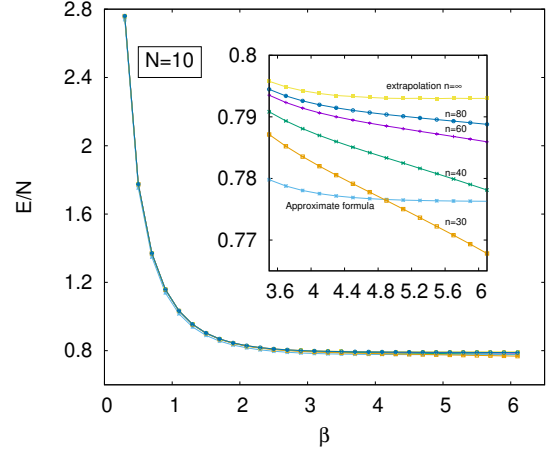


Figure 4.  $N = 10$ . Average energy  $E/N$  as a function of  $\beta$  obtained with PIMC and compared with that obtained with our approximate formula for the partition function. The PIMC energy curves for  $n = 30, 40, 60$  and  $80$  are displayed together with the extrapolated curve at  $n = \infty$ . The inset is a magnified view of the low-temperature regime.

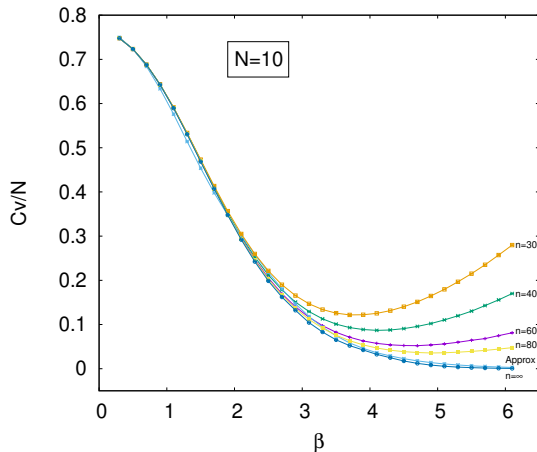


Figure 5.  $N = 10$ . Specific heat  $c_v/N$  as a function of  $\beta$  obtained with PIMC and compared with that obtained with our approximate formula for the partition function. The PIMC energy curves for  $n = 30, 40, 60$  and  $80$  are displayed together with the extrapolated curve at  $n = \infty$ .

#### IV. CONCLUSIONS

In this work, we have derived a general approximate expression for the partition function of an arbitrary number of coupled quantum oscillators. Evaluating this expression requires solving a system of nonlinear coupled equations, the size of which scales with the number of parameters in the potential energy function. For simple systems involving up to  $N = 10$  coupled oscillators, numerical tests using a simple iterative scheme consistently yield to a stable and unique solution, provided that reasonable initial conditions are chosen. Quantitatively, the resulting thermodynamic quantities -free energy, average energy, and specific heat- are found to be quite accurate, with relative errors typically within a few percent, even at low temperatures.

Extending this approach to more realistic systems, particularly those with a significantly larger number of oscillators, is certainly the main challenge for future work. Preliminary results indicate that convergence issues may arise for such systems, indicating that the use of more

advanced numerical algorithms to ensure stability will be probably necessary. Additionally, the high computational cost associated with evaluating the covariance matrix, which involves  $N$ -dimensional integrals, may become a limiting factor. This limitation could potentially be removed by modifying the criterion used to fit the exact potential with a Gaussian distribution (see Eq. 4), thus circumventing the need for explicit covariance matrix evaluation.

Finally, let us note that a particularly promising application of our formula is the computation of the rovibrational partition function of large (bio)molecules. Realizing this, however, requires extending the formalism to deal with the more complex kinetic energy operators expressed in internal coordinates. Initial developments in this direction are encouraging and suggest that such a generalization is feasible.

#### ACKNOWLEDGMENTS

I would like to thank Dr. A. Scemama for interesting discussions and valuable help with the simulations. I also thank the Centre National de la Recherche Scientifique (CNRS) for its continued support. This work used the HPC resources from CALMIP (Toulouse) under allocation 2025-18005. I acknowledge funding from the European Research Council (ERC) under the European Union's Horizon 2020 research and innovation programme (Grant agreement No. 863481).

#### Appendix A: Two useful formulas

As a first formula, let us show that

$$\sum_{i=1}^n \frac{\left(\sum_j O^{ij}\right)^2}{\lambda_i + \tau^2 x} = \frac{n^2}{\beta \tau x} \quad (\text{A1})$$

This formula is easy to derive by remarking that the matrix  $A$ , which is invariant by translation, admits as one of its eigenstates the constant normalized vector, say  $u_1 = \left(\frac{1}{\sqrt{n}}, \dots, \frac{1}{\sqrt{n}}\right)$  with eigenvalue  $\lambda_1 = 0$ . As a consequence, we have

$$\sum_{j=1}^n O^{1j} = \sum_{j=1}^n u_{1j} = \sqrt{n}$$

The columns of the matrix  $O^{ij}$  being orthogonal we have

$$\sum_{j=1}^n O^{ij} = 0 \text{ for } i \neq 1.$$

Using this relation, only the component  $i = 1$  of the sum in Eq.(A1) is not vanishing, thus leading to the desired equality.

As a second useful formula, let us first show that the quantity  $\mathcal{A}$  defined as

$$\mathcal{A} = \sum_{k=1}^N \frac{b_{gk}^2}{\omega_{gk}^2} - 2 \sum_{1 \leq k < l \leq N} K_{gkl} \bar{x}_k \bar{x}_l + \sum_{k=1}^N \frac{(\sum_l \bar{K}_{gl} S_{kl})^2}{\Omega_{gk}^2} \quad (\text{A2})$$

is equal to the more simple expression

$$\mathcal{A} = (b_g, M^{-1} b_g)$$

where

$$M_{kl} = \omega_{gk}^2 \delta_{kl} + K_{gkl}. \quad (\text{A3})$$

Let us first evaluate the third term of the R.H.S of Eq.(A2). Defining the quantity  $X$  as follows

$$X \equiv \sum_{k=1}^N \frac{\sum_{l=1}^N \bar{K}_{gl} S_{lk}^T}{\Omega_{gk}^2} \quad (\text{A4})$$

and using Eq.(28) we have

$$X = \sum_{l,m,i,j} \left( \frac{\sum_{k=1}^N S_{lk}^T S_{mk}^T}{\Omega_{gk}^2} \right) K_{gli} K_{gmj} \bar{x}_i \bar{x}_j.$$

Using the fact that

$$\frac{\sum_{k=1}^N S_{lk}^T S_{mk}^T}{\Omega_{gk}^2} = M_{lm}^{-1}$$

and the expression of the matrix  $M$ , Eq.(A3), we get

$$X = \sum_{i,j} (M_{ij} - \delta_{ij} \omega_{gj}^2 - \delta_{ij} \omega_{gi}^2 + M_{ij}^{-1} \omega_{gi}^2 \omega_{gj}^2) \bar{x}_i \bar{x}_j$$

Now, using the definition of  $\bar{x}_i$ , Eq.(27), we get

$$X = (\bar{x}, M \bar{x}) - 2 \sum_i \frac{b_{gi}^2}{\omega_{gi}^2} + \sum_{i,j} b_{gi} M_{ij}^{-1} b_{gj}.$$

Putting this expression into expression (A2) for  $\mathcal{A}$  we obtain our final formula

$$\mathcal{A} = (b_g, M^{-1} b_g)$$

## Appendix B: Path Integral Monte Carlo

Path Integral Monte Carlo (PIMC) is a standard numerical method for computing quantum thermodynamic

properties; for a detailed presentation, see *e.g.* [15]. In our implementation we use a Fourier representation for the paths, a way of generating preferentially paths with large scale deformations and, thus, an improved convergence for the estimators[13],[34],[35]. Using the notations of this work, Fourier modes are realized here by drawing independently the transformed variables  $\tilde{x}_k^i = \sum_{j=1}^n O^{ij} x_k^j$  resulting from the diagonalization of the kinetic matrix  $A$ , Eq.(15). The probability density function is given by

$$\pi(\tilde{x}_k^i) \sim e^{-\frac{\lambda_i}{\tau} \tilde{x}_k^{i2}}. \quad (\text{B1})$$

In PIMC various estimators can be employed for computing the average energy and specific heat. Here, we use the following low-variance estimators. For the average energy  $E$  we use the so-called centroid virial estimator given by[36],[37]

$$E = \langle \epsilon_{CV} \rangle = \frac{N}{2\beta} + \frac{1}{2} \langle \bar{W}_1 \rangle + \langle \bar{V} \rangle \quad (\text{B2})$$

where

$$\bar{V} = \frac{1}{n} \sum_{i=1}^n V(\mathbf{x}^i) \quad (\text{B3})$$

and

$$\bar{W}_1 = \frac{1}{n} \sum_{i=1}^n \sum_{k=1}^N (x_k^i - \bar{x}_k) \frac{\partial V}{\partial x_k}(\mathbf{x}^i) \quad (\text{B4})$$

with

$$\bar{x}_k = \frac{1}{n} \sum_{i=1}^n x_k^i. \quad (\text{B5})$$

For the specific heat, we use the so-called double centroid virial estimator given by[36],[37]

$$c_v = \beta^2 \left[ \langle \epsilon_{CV}^2 \rangle - \langle \epsilon_{CV} \rangle^2 - \frac{1}{4\beta} \langle 3\bar{W}_1 + \bar{W}_2 \rangle \right] \quad (\text{B6})$$

with

$$\bar{W}_2 = \frac{1}{n} \sum_{i=1}^n \sum_{k,l=1}^N (x_k^i - \bar{x}_k) (x_l^i - \bar{x}_l) \frac{\partial^2 V}{\partial x_k \partial x_l}(\mathbf{x}^i) \quad (\text{B7})$$

- 
- [1] C. Banwell and E. McCash. *Fundamentals for Molecular Spectroscopy 4th Edition*. Mc Graw Hill, 1994.  
 [2] G. P. Srivastava. *The Physics of Phonons*. Taylor & Francis, London, 1990.

- [3] Robert W. Boyd. *Nonlinear Optics*. Academic Press, Cambridge, MA, 4 edition, 2020.  
 [4] Michael E. Peskin and Daniel V. Schroeder. *An Introduction to Quantum Field Theory*. Westview Press, Boulder,

- CO, 1995.
- [5] Wojciech H. Zurek. Decoherence, einselection, and the quantum origins of the classical. *Reviews of Modern Physics*, 75(3):715–775, 2003.
  - [6] M. Kjaergaard, M. E. Schwartz, J. Braumüller, P. Krantz, J. I.-J. Wang, S. Gustavsson, and W. D. Oliver. Superconducting qubits: Current state of play. *Annual Review of Condensed Matter Physics*, 11:369–395, 2020.
  - [7] Fritz Haake. *Quantum Signatures of Chaos*. Springer, Berlin, 3 edition, 2010.
  - [8] Jingrui Li, Clemens Woywod, Valérie Vallet, and Christoph Meier. Investigation of the dynamics of two coupled oscillators with mixed quantum-classical methods. *The Journal of Chemical Physics*, 124(18):184105, 05 2006.
  - [9] Daniel T. Colbert and William H. Miller. A novel discrete variable representation for quantum mechanical reactive scattering via the s-matrix kohn method. *The Journal of Chemical Physics*, 96(3):1982–1991, 1992.
  - [10] Hans-Dieter Meyer, Fabien Gatti, and Graham A. Worth, editors. *Multidimensional Quantum Dynamics: MCTDH Theory and Applications*. Wiley-VCH, Weinheim, Germany, 2009.
  - [11] Alberto Baiardi, Christopher J. Stein, Vincenzo Barone, and Markus Reiher. Vibrational density matrix renormalization group. *Journal of Chemical Theory and Computation*, 13(8):3764–3777, 2017.
  - [12] Nina Glaser, Alberto Baiardi, and Markus Reiher. Flexible dmrg-based framework for anharmonic vibrational calculations. *Journal of Chemical Theory and Computation*, 19(24):9329–9343, 2023. PMID: 38060309.
  - [13] Richard P. Feynman. *Statistical Mechanics: A Set of Lectures*. W. A. Benjamin, Reading, Massachusetts, 1972. Lectures originally delivered at Caltech.
  - [14] Hagen Kleinert. *Path Integrals in Quantum Mechanics, Statistics, Polymer Physics, and Financial Markets*. World Scientific, Singapore, 5th edition, 2009.
  - [15] David M. Ceperley. Path integrals in the theory of condensed helium. *Reviews of Modern Physics*, 67(2):279–355, 1995.
  - [16] Dominik Marx and Michele Parrinello. Ab initio path integral molecular dynamics: Basic ideas. *The Journal of Chemical Physics*, 104(11):4077–4082, 1996.
  - [17] Michele Ceriotti, Michele Parrinello, Thomas E. Markland, and David E. Manolopoulos. Accelerating the convergence of path integral dynamics with a generalized langevin equation. *The Journal of Chemical Physics*, 134(8):084104, 2011.
  - [18] Michel Caffarel. Path integral for the quartic oscillator: an accurate analytic formula for the partition function. *Journal of Mathematical Chemistry*, 63:353–382, 2025.
  - [19] Michel Caffarel. Analytic model for the energy spectrum of the anharmonic oscillator. *Physics Letters A*, 525:129925, 2024.
  - [20] Carl M. Bender and Tai Tsun Wu. Anharmonic oscillator. *Phys. Rev.*, 184:1231–1260, Aug 1969.
  - [21] Carl M. Bender and Tai Tsun Wu. Large-order behavior of perturbation theory. *Phys. Rev. Lett.*, 27:461–465, Aug 1971.
  - [22] P. M. Stevenson. Optimized perturbation theory. *Phys. Rev. D*, 23:2916–2944, Jun 1981.
  - [23] J. C. Wrigley. An alternative implementation of the "principle of minimal sensitivity". *Phys. Rev. D*, 27:1965–1967, Apr 1983.
  - [24] S K Kauffmann and S M Perez. Minimal sensitivity optimisation of perturbative wavefunctions. *Journal of Physics A: Mathematical and General*, 17(10):2027, jul 1984.
  - [25] Anna Okopińska. Nonstandard expansion techniques for the effective potential in  $\lambda\phi^4$  quantum field theory. *Phys. Rev. D*, 35:1835–1847, Mar 1987.
  - [26] Philip M. Morse. Diatomic molecules according to the wave mechanics. ii. vibrational levels. *Physical Review*, 34(1):57–64, 1929.
  - [27] L. D. Landau and E. M. Lifshitz. *Quantum Mechanics: Non-Relativistic Theory*, volume 3 of *Course of Theoretical Physics*. Pergamon Press, Oxford, 3rd edition, 1977.
  - [28] Neil W. Ashcroft and N. David Mermin. *Solid State Physics*. Harcourt College Publishers, New York, 1976.
  - [29] Pierre Ramond. *Field Theory: A Modern Primer*. Westview Press, Boulder, CO, 2nd edition, 1990.
  - [30] Philip J. Davis. *Circulant Matrices*. AMS Chelsea Publishing, Providence, RI, 2nd edition, 1994.
  - [31] Daniel Shanks. Non-linear transformations of divergent and slowly convergent sequences. *Journal of Mathematics and Physics*, 34(1-4):1–42, 1955.
  - [32] Felix Uhl, Dominik Marx, and Michele Ceriotti. Accelerated path integral methods for atomistic simulations at ultra-low temperatures. *The Journal of Chemical Physics*, 145(5):054101, 08 2016.
  - [33] Michele Ceriotti, Michele Parrinello, Thomas E. Markland, and David E. Manolopoulos. Efficient stochastic thermostating of path integral molecular dynamics. *The Journal of Chemical Physics*, 133(12):124104, 09 2010.
  - [34] J. D. Doll. Monte carlo fourier path integral methods in chemical dynamics. *The Journal of Chemical Physics*, 81(8):3536–3541, 10 1984.
  - [35] Jimmie D. Doll and David L. Freeman. A monte carlo method for quantum boltzmann statistical mechanics. *The Journal of Chemical Physics*, 80(5):2239–2240, 03 1984.
  - [36] Motoyuki Shiga and Wataru Shinoda. Calculation of heat capacities of light and heavy water by path-integral molecular dynamics. *The Journal of Chemical Physics*, 123(13):134502, 09 2005.
  - [37] Sabry G. Moustafa and Andrew J. Schultz. Generalized path integral energy and heat capacity estimators of quantum oscillators and crystals using harmonic mapping. *Journal of Chemical Theory and Computation*, 20(22):10132–10146, 2024.